Molecular dynamics investigation of the thermomechanical behavior of monolayer GaN

J. V. N. Sarma, Rajib Chowdhury, and R. Jayaganthan

Citation: J. Appl. Phys. **113**, 243504 (2013); doi: 10.1063/1.4812328
View online: http://dx.doi.org/10.1063/1.4812328
View Table of Contents: http://jap.aip.org/resource/1/JAPIAU/v113/i24
Published by the AIP Publishing LLC.

JOURNAL OF APPLIED PHYSICS **113**, 243504 (2013)

Molecular dynamics investigation of the thermomechanical behavior of monolayer GaN

J. V. N. Sarma,[1,a)] Rajib Chowdhury,[2,b)] and R. Jayaganthan[3,c)]
[1]*Center of Nanotechnology, Indian Institute of Technology Roorkee, Roorkee 247 667, India*
[2]*Department of Civil Engineering, Indian Institute of Technology Roorkee, Roorkee 247 667, India*
[3]*Department of Metallurgical and Materials Engineering and Center of Nanotechnology, Indian Institute of Technology Roorkee, Roorkee 247 667, India*

(Received 11 April 2013; accepted 10 June 2013; published online 26 June 2013)

Molecular dynamics simulations are performed on monolayer gallium nitride to study their mechanical behavior at various temperatures in the range of 10 to 1700 K. The transition from brittle to ductile nature has been illustrated from the evolution of fracture at two different temperatures of 700 and 1300 K. Brittle to ductile transition temperatures T_{BDT} are obtained from the plots of logarithm of yield stress and inverse temperature at different strain rates and compared qualitatively with the same system in the presence of single and diatomic vacancies. Logarithm of strain rate against inverse of T_{BDT} thus obtained represents an Arrhenius plot, the slope of which corresponds to the activation energy of dislocation glide that is found to be approximately 2.0 ± 0.05 eV for the present case. This suggests that the brittle to ductile transition is controlled by the dislocation mobility as in the case of other semiconductors like silicon and germanium. This behavior is found to be consistent with the presented underlying models. In addition, thermal conductivities are obtained over a temperature range of 300 to 2000 K from the equilibrium Green-Kubo formulations and compared with the (25,0) nanotube that is generated from the same system of monolayer GaN. The values are found to be decreased in both the cases as compared to the bulk gallium nitride, and the reduction in the values of thermal conductivity can be attributed to the finite size effects, increased surface inelastic scattering, and change of phonon spectrum at low dimensions, respectively. © *2013 AIP Publishing LLC*. [http://dx.doi.org/10.1063/1.4812328]

I. INTRODUCTION

Monolayer inorganic nanostructures such as boron nitride (BN),[1–3] zinc oxide (ZnO),[4,5] and transition metal oxides[6,7] are showing upcoming interests in the research community in recent years as that of graphene monolayers,[8] mainly due to their special characteristic properties at the nanoscale and amazing functionalities for wide applications in the nanoelectronics and sensor industry.[9–12] The successful synthesis of single walled nanotubes of gallium nitride (GaN) by "epitaxial casting"[13] and also the formation of monolayers of BN and ZnO strongly suggests the possibility of experimental existence of monolayer GaN (GaN-ML) in the very near future. Recently, Yeh *et al.*[14] have reported the application of monolayer GaN as growth templates for light emitting diodes. GaN nanostructures of low thermal conductivity κ could be advantageous in nanoscale energy harvesting devices,[15] due to their increased figure of merit. Wang *et al.*[16] have calculated the brittle to ductile transition temperatures for GaN nanotubes under different applied strain rates. They later applied nonequilibrium molecular dynamics (MD) simulations to obtain the κ of GaN nanotubes along the tube axis and found the value to be in the order of few tens of W/mK at 600 K.[17] Single crystalline GaN nanotubes were also studied for their transport properties using *ab-initio* techniques.[18] Based on the first-principle calculations, Chen *et al.*[19] studied the band gap engineering in GaN-ML by chemical modification and under external electric field. By using analytical formulations, the effective mechanical properties of hexagonal-BN monolayers were predicted by Boldrin *et al.*,[20] which agreed well with the other simulation and experimental approaches. Sarma *et al.*[21] have recently obtained the mechanical behavior of GaN-ML under uniaxial tension using molecular dynamics. Although some reports exist on the thermal properties of GaN nanotubes, especially the thermomechanical behavior of GaN-ML has been rarely investigated, in spite of its important applications.

In this paper, MD simulations are performed using Stillinger-Weber (SW) potential on a system of GaN-ML, which resembles graphene monolayer with carbon atoms replaced by alternating gallium (Ga) and nitrogen (N) atoms. More details on the structure of GaN-ML can be found elsewhere.[19,21] The SW form of potentials has been successfully employed in recent years on GaN nanostructures.[16,17,21,22] We investigated the mechanical behavior of such a system at different initial temperatures and obtained the brittle to ductile transition temperatures as a function of applied tensile strain rate. Evolution of fracture at selected temperatures has been illustrated to confirm this transition. Equilibrium Green-Kubo (GK) formulations are employed to obtain thermal conductivity at the simulated temperatures and compared with (25,0) nanotube that is generated from the same GaN-ML.

[a)]Electronic mail: jvnano11@gmail.com
[b)]Electronic mail: rajibfce@iitr.ernet.in
[c)]Electronic mail: rjayafmt@iitr.ernet.in

II. MODELING AND SIMULATION

Molecular dynamics code LAMMPS[23] has been used in this work. The parameters provided by Bere and Serra[24] for the SW potential[25] to describe the force fields between gallium and nitrogen atoms were employed on a system of square shaped GaN-ML of nearly 8.5 nm in length that accommodates 1450 atoms. This form of empirical potentials was proven to be robust even in the presence of point and line defects for the GaN system. The system was considered to be canonical and the constant temperature was maintained by applying Nose'-Hoover thermostat.[26] With a time step of $\Delta t = 0.5$ fs, the equations of motion through time were solved using the Velocity-Verlet integration algorithm. The system was initially brought to equilibrium configuration by a relaxation process for $s = 2 \times 10^4$ steps.

To investigate the effect of temperature on the mechanical behavior of GaN-ML, the temperature was varied from 10 to 1700 K at a constant strain rate of 0.89%/ps. Uniaxial tensile loading was applied at this strain rate at one of the ends, keeping the other end fixed. The axial stress $\sigma_y(t)$ was taken to be the arithmetic average of the local stresses on all atoms, normalized to actual volume from that of the simulation cell volume. If ε_y is the strain, the strain rate is given by: $\dot{\varepsilon} = \varepsilon_y / s\Delta t$. As the lifetime τ of a loaded solid, defined as the time taken before its breakdown, is mainly determined by the stress and temperature, it is essential to study the variation of fracture strength σ_y with temperature T. Fracture is initiated when Bailey's integral,[27] i.e., the principle of linear summation of partial fracture is satisfied

$$\int_0^{t_f} \frac{dt}{\tau[\sigma_y(t), T]} = 1, \tag{1}$$

where t_f is the fracture time. The lifetime $\tau[\sigma_y(t), T]$ was shown to follow the universal Arrhenius relation[28]

$$\tau = \tau_0 \exp\left(\frac{U_0 - \gamma\sigma_y}{k_B T}\right), \tag{2}$$

where τ_0 is natural vibration period of atoms, U_0 is the atomic binding energy, which is the activation energy for fracture, $\gamma = q\sigma_y V$, where q is the coefficient of local over stresses and V is the activation volume, which is related to molecular structural disorientation, and k_B is the Boltzmann constant. This Maxwell-Boltzmann distribution shows that the energy barrier $(U_0 - \gamma\sigma_y)$ and the temperature T determine the life time τ. Substituting Eq. (1) into Eq. (2), we have

$$\sigma_f(T) = \frac{U_0}{\gamma} + \frac{k_B}{\gamma} \ln\left(\frac{\gamma E \dot{\varepsilon} \tau_0}{k_B T}\right) T, \tag{3}$$

where $E = \sigma_y / \varepsilon_y$ is the Young's modulus and $\sigma_f = E\dot{\varepsilon} t_f$, for a linear elastic solid. Since the logarithmic multiplier slightly depends on the fluctuations in γ, $\dot{\varepsilon}$ and T, it can be assumed to be constant.[29] Thus, Eq. (3) may be simplified as

$$\sigma_f(T) = A + B \times T, \tag{4}$$

where $A \equiv \frac{U_0}{\gamma}; B \equiv \frac{k_B}{\gamma} \ln\left(\frac{\gamma E \dot{\varepsilon} \tau_0}{k_B T}\right)$. Equation (4) predicts that the fracture stress changes linearly with the temperature with an intercept on the stress axis, provided $\gamma =$ constant and $U_0 =$ constant. To further understand the effect of temperature on crack propagation, we apply quantized fracture mechanics (QFM)[30] which assumes that fracture of small systems with a given geometry and type of loading occurs at "quantized" stresses, in contrast to classical continuum methods like Griffith's criterion and stress-intensity factor based methods. QFM considers the quantum nature of solid at atomic scale and takes into account the underlying crystal structure by substituting the differentials in the Griffith's criterion with finite differences. Considering mode I loading and blunt crack, i.e., chains of removed atoms in the case of nanostructures, on a finite width $(2w)$ plate, if $2l$ is the crack length and ρ is the tip radius of the crack, the failure strength can be predicted as[31]

$$\sigma_f(l, \rho) = \sigma_c(\dot{\varepsilon}, T) \sqrt{\frac{1 + \rho/2a}{1 + 2l/a}} \left[\frac{2w}{\pi l} \tan\left(\frac{\pi l}{2w}\right)\right]^{1/2}, \tag{5}$$

where σ_c is the ideal strength of the defect-free material and a is the fracture quantum which is the minimum extension of the crack per one interatomic bond breaking along the crack propagation direction. In the case of a defect-free structure, $\sigma_f = \sigma_c$ since, $2L = 0$, and $\rho = 0$. Such a dependence of fracture strength on thermal activation energy and temperature suggests the transition from brittle to ductile nature of GaN-ML at some particular temperature for a given strain rate. At a constant strain rate, the yielding of a crystal is a thermally activated process that mainly occurs by the generation and glide of dislocations.[32] The activation enthalpy for such a process is expressed by

$$\Delta H = -T \times V \left(\frac{\partial \tau_y}{\partial T}\right) \dot{\varepsilon}, \tag{6}$$

where the activation volume V can be written as

$$V = k_B T \left(\frac{\partial(\ln \dot{\varepsilon})}{\partial \tau_y}\right)_T. \tag{7}$$

The yield stress τ_y can be related to the activation enthalpy as

$$\tau_y = A\dot{\varepsilon}^{1/n} \exp\left(\frac{\Delta H}{k_B T}\right), \tag{8}$$

where A and n are constants such that $n\Delta H = \Delta H_d$ is approximately the activation energy for the dislocation glide. Then, the temperature independent fracture strength $\sigma_f = \tau_f / S$, S being the geometrical parameter, and the brittle to ductile transition temperature T_{BDT} are related through activation enthalpy, using Eq. (8) as

$$T_{BDT} = \frac{\Delta H}{k_B \ln\left(\frac{S\sigma_f}{A\dot{\varepsilon}^{1/n}}\right)}, \tag{9}$$

which can be rearranged as

$$\ln(\dot{\varepsilon}) = (-\Delta H_d/k_B)1/T_{BDT} + n\ln(S\sigma_f/A). \quad (10)$$

This represents a straight line for $\ln(\dot{\varepsilon})$ versus $1/T_{BDT}$ plot with a slope of $\Delta H_d/k_B$ and an intercept of $n\ln(S\sigma_f/A)$. We obtained the values of T_{BDT} for different strain rates: $\dot{\varepsilon} = 0.1, 0.4, 0.89, 1.6$, and 2.5%/ps that are calculated as described above.

Thermal conductivity can be obtained from equilibrium molecular dynamics using GK equations, steady state nonequilibrium simulations, and nonequilibrium molecular dynamics simulations. The latter two formulations are based on the nonequilibrium thermodynamics, while the GK method relies on the calculations of per atom potential and kinetic energies and per-atom stress tensor in a steady-state equilibrated simulation. We choose to employ GK approach, as it is believed to give fairly accurate results, although at the expense of longer simulation times. The GK formulas relate the ensemble average of the auto-correlation of the heat flux J to the thermal conductivity κ

$$\begin{aligned} J &= \frac{1}{V}\left[\sum_i e_i\vec{v}_i - \sum_i S_i\vec{v}_i\right] \\ &= \frac{1}{V}\left[\sum_i e_i\vec{v}_i + \sum_{i<j}(\vec{f}_{ij}.\vec{v}_j)\vec{X}_{ij}\right] \\ &= \frac{1}{V}\left[\sum_i e_i\vec{v}_i + \frac{1}{2}\sum_{i<j}(\vec{f}_{ij}.(\vec{v}_i+\vec{v}_j))\vec{X}_{ij}\right] \end{aligned} \quad (11)$$

which indicates the energy conservation with e_i being the per atom energy (kinetic and potential) and S_i being the per-atom stress tensor. The thermal conductivity is then obtained by

$$\begin{aligned} \kappa &= \frac{V}{k_B T^2}\int_0^\infty \langle J_x(0)J_x(t)\rangle dt \\ &= \frac{V}{3k_B T^2}\int_0^\infty \langle \vec{J}(0).\vec{J}(t)\rangle dt\,. \end{aligned} \quad (12)$$

Initial temperatures on the GaN-ML are taken from 300 to 2000 K in steps and the corresponding thermal conductivities are obtained through simulation. The procedure is repeated with a single walled nanotube generated from the same GaN-ML, for comparison.

III. RESULTS AND DISCUSSION

Fig. 1 illustrates the variation of tensile stress versus strain at different temperatures from 10 K to 1700 K, at a constant strain rate of 0.89%/ps. A linear elastic behavior that follows Hooke's law can be seen at all simulated temperatures except at higher temperatures. At room temperature, the critical stress and strain of the GaN-ML are found to be 19.08 GPa and 4.8%, respectively, giving rise to a tensile strength of 0.411 TPa. Thus, the initial brittleness of monolayer GaN is observed to be smaller than the graphene sheet, which could be due to the decreased bond strength among the Ga-Ga, N-N, and Ga-N bonds as compared to the C-C bond. At higher temperatures, a zig-zag type of variation could be observed as represented in the inset, which indicates that the monolayer fails in a brittle manner at low temperatures and in a ductile manner at higher temperatures. The critical stress can be observed to be much lower at higher temperatures than at low temperatures, which confirms the role of thermally activated process in the elastic behavior of monolayer GaN, because with increase in the temperature, large number of atoms gain sufficient energies to overcome the energy barrier $(U_0 - \gamma\sigma_y)$.

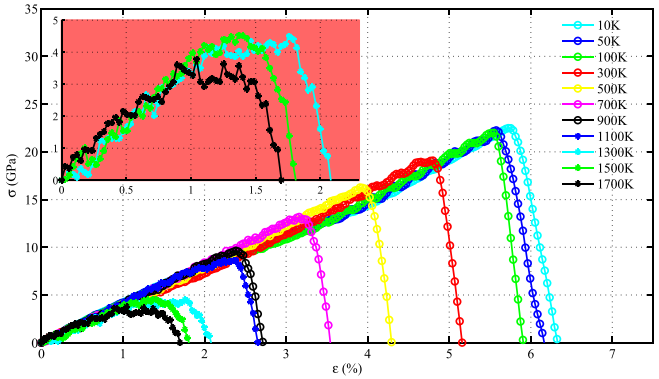

FIG. 1. Stress-strain response of GaN-ML at different temperatures in the range of 10 to 1700 K at a strain rate of 0.89%/ps. The linear behavior indicates the elastic nature, except for the higher temperatures. A zig-zag type of variation of the response at higher temperatures is shown in the inset. This indicates the transition to ductile nature at higher temperatures.

The fracture evolution as captured at the simulation temperatures of 700 K and 1300 K for a given strain rate of 0.89%/ps is given in Fig. 2. The blue and red atoms indicate N and Ga atoms, respectively. The corresponding values of fracture stress and strain are also shown at different rupture incidents during fracture. It can be seen that, at lower temperatures before fracture, the crack propagates with a clean cut by the formation of atomic vacancies, which indicates the failure in brittle manner. At the temperature close to T_{BDT}, initiation of the formation of a group of chain of atoms with a clear necking that link two separated portions before fracture could be observed. The reason for such a necking of atoms being, at some temperature around this particular temperature, the brittle to ductile transition has occurred for a given strain rate and the applied tensile loading no longer suffices for the propagation of the crack tip. The emitted dislocations from the tip make it blunt, thereby shielding the tip from the applied loading, resulting in the necking of atoms. The negative values of corresponding stresses further confirm this shielding by compressing the group of atoms due to higher temperature.

The initial location of the crack depends on several parameters, such as the direction of applied loading, the strain rate, geometry of the structure, and most importantly the boundary conditions. Too low strain rate has an effect of making the tensile behavior quasi-static at the same time at the expense of computational cost, while too high strain rate alters the accuracy of the tensile behavior itself. The nature of boundary conditions dramatically changes the location of the crack. With the applied periodic boundary conditions in

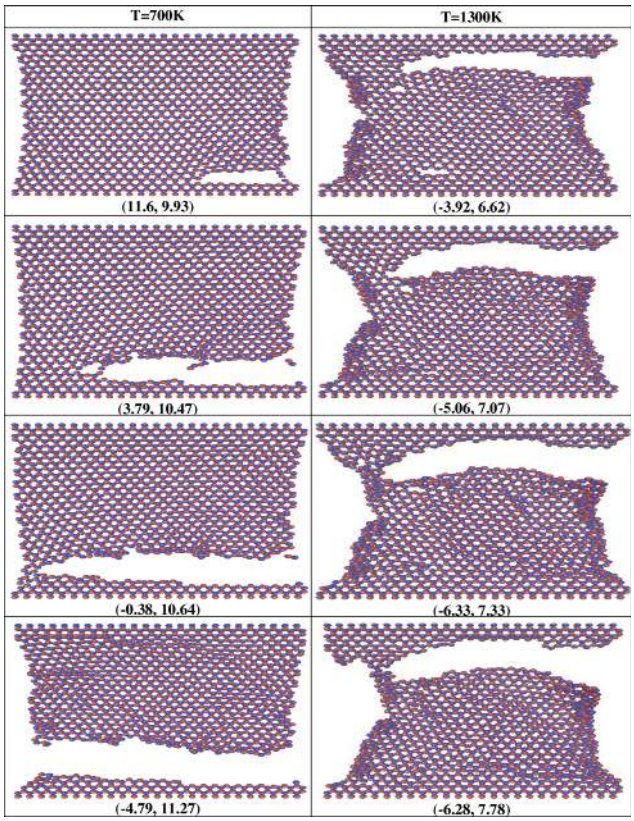

FIG. 2. The fracture process at 700 K and 1300 K. The values in the parentheses are the critical stress (in GPa) and strain (in%), respectively, at that particular instant of fracture time. At 700 K, the fracture occurs with a clear cut, indicating the brittle nature while at 1300 K which is close to T_{BDT} for this strain rate, the formation of a group of atoms as a chain that links the separated portions can be seen. The negative values of corresponding stresses represent the compression of the group of atoms due to higher temperature.

the present work, a slight deviation in the initial origin of crack from the location of half the length of the sheet, as is normally expected for a mode I Griffith's crack, could be observed in Fig. 2. However, the criterion that the propagation of the crack plane is normal to the plane of the direction of applied stress is fulfilled very well in the case of brittle failure as observed at 700 K, and thus could be still regarded as mode I Griffith's crack, irrespective of where the actual origin of the crack location on the longitudinal axis. However, in the case of a ductile failure as observed in the case of 1300 K, a mixed mode I and mode II failure, i.e., crack plane growing at an angle of 60° to the applied stress direction and also a much blunt crack tip can be noticed, further confirming the transition to ductile behavior at some higher temperature. Such observations of slight deviation from the expected location of crack were also noticed earlier for graphene and BN monolayers.[33,34]

The values of critical stress for the pristine GaN-ML are obtained from Fig. 1. The variation of critical stress thus obtained can be seen in Fig. 3 as a function of temperature. In the simulated range of initial temperatures, the critical stress decreases linearly with increasing temperatures. This indicates the transition from brittle to ductile nature at higher temperatures. This behavior is also in accordance with the prediction of Eq. (4). The stress versus strain simulations in

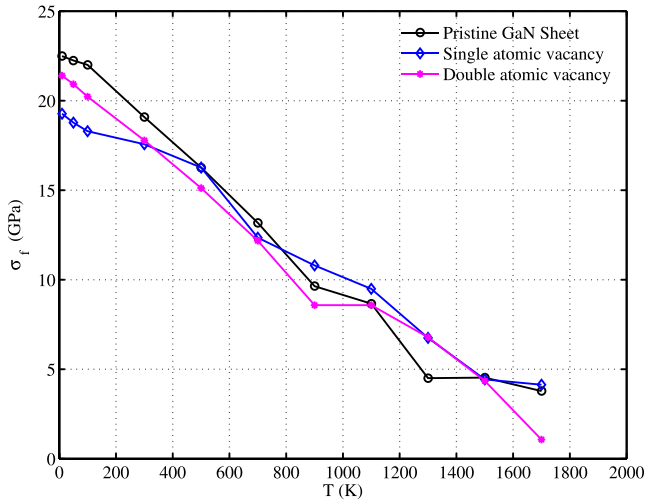

FIG. 3. The variation of critical stress with temperature is shown. The critical stress decreases linearly with increasing temperature, in confirmation with the prediction of Eq. (4). For comparison, the curves are obtained with the GaN-ML having single and double vacancies. All the three cases exhibit the similar qualitative behavior, although there are quantitative differences. A reduction in the critical stress of the GaN-ML in the presence of atomic vacancies is also evident. In all the three cases, a kink can be observed at higher temperatures, indicating the brittle to ductile transition.

the same range of initial temperatures are repeated with the GaN-ML in the presence of single and double atomic vacancies. For comparison, the values of critical stress thus obtained against the temperature are also plotted in Fig. 3 for both the cases. Qualitatively, all the three cases exhibit the similar linear behavior, although there are quantitative differences. The reduction in the values of initial critical stress due to the presence of atomic vacancies is also evident. This reduction in the strength of the GaN-ML may be due to the fact that the vacancies act as centers for the initiation of the crack and the atoms around the vacancy experiences reduced atomic coordination, giving rise to the fracture at a much earlier time step than the one with pristine GaN-ML. In all the three cases, a kink can be observed at higher temperatures that corresponds to a critical temperature T_c and a critical stress σ_c, indicating the brittle to ductile transition around that particular temperature. Kink-diffusion model[35] suggests that the variation of yield stress with temperature can be represented by plotting $\ln(\tau_y)$ versus $1/T$. This is shown in Fig. 4(a), where $\ln(\tau_y)$ increases with increase in temperature. However, an abrupt change in the slope can be observed at a critical temperature T_c. The occurrence of changes in the slope is represented in the inset. The different slopes at high temperature $T > T_C$ and low temperature $T < T_C$ regimes, respectively, correspond to two different activation enthalpies H_1 and H_2 for dislocation glide. Such features of formation of a kink in the critical stress versus temperature plots and the change of slopes at low and high temperature regime are qualitatively very similar to the experimental observations for bulk GaN crystal.[36] The interesting advantage of such a plot is the direct prediction of fracture stress and T_{BDT} without any fracture measurements. The simulations are repeated for GaN-ML in the presence of single and diatomic vacancies under the same strain rate. It can be seen that T_{BDT} falls nearly at the same point in all the three cases. This is as

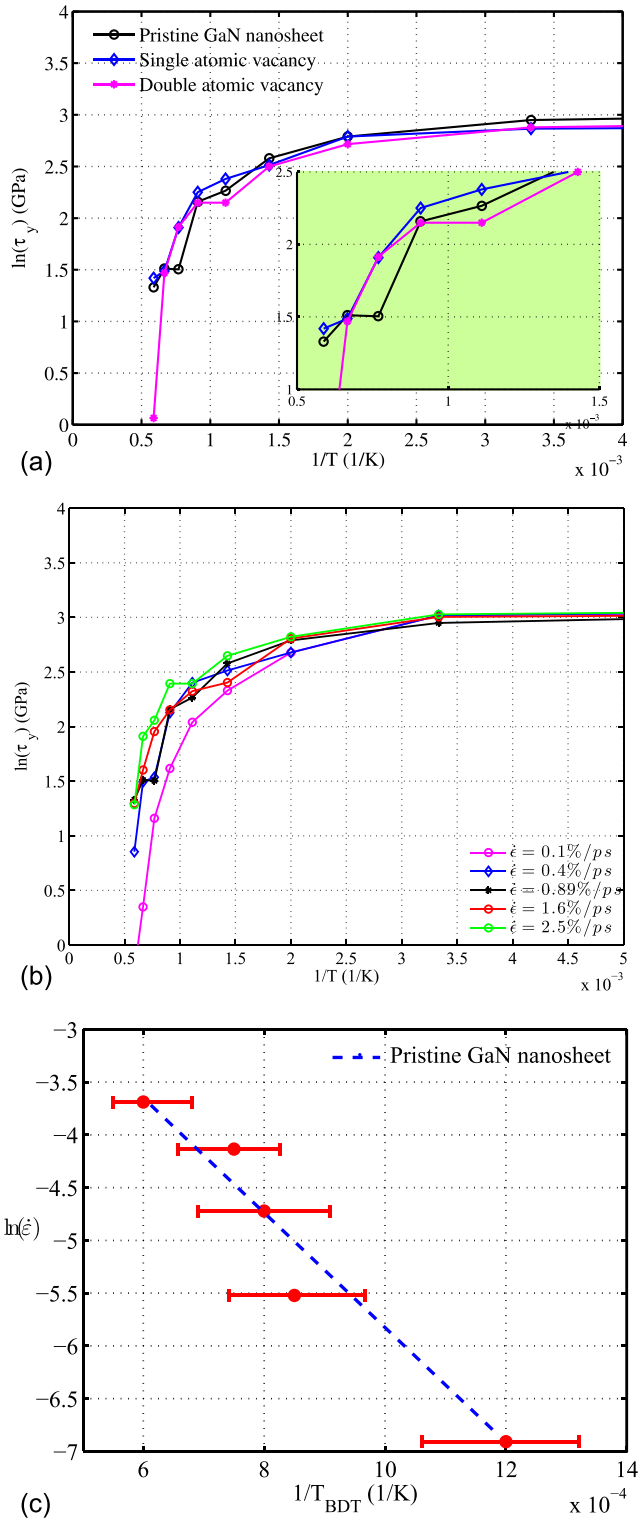

FIG. 4. (a) The variation of $\ln(\tau_y)$ as a function of inverse temperature at a strain rate of 0.89%/ps. The temperature at which an abrupt change in the slope of the curve occurs corresponds to T_{BDT}. The occurrence of change of slopes at high temperatures is shown in the inset. The results are compared for GaN-ML with single and diatomic vacancies. It can also be seen that T_{BDT} falls nearly at the same point in all the three cases, as the fraction of vacant atoms in the GaN-ML is much lesser as compared to the total number of atoms in the GaN-ML; (b) the variation of $\ln(\tau_y)$ as a function of inverse temperature at strain rates of 0.1, 0.4, 0.89, 1.6, and 2.5%/ps. The corresponding values of T_{BDT} are obtained, as shown in Table I; (c) variation of $\ln\dot{\varepsilon}$ vs. $1/T_{BDT}$. The value of T_{BDT} shifts to the higher values with the increase in rate of applied tensile loading. The linear dependency is consistent with the prediction of Eq. (10).

expected, because the fraction of vacancy atoms present is much lesser as compared to the total number of atoms. T_{BDT} can be deduced from such plots and the values of T_{BDT} thus obtained for pristine GaN-ML by means of Fig. 4(b) for different strain rates of $\dot{\varepsilon} = 0.1, 0.4, 0.89, 1.6$, and 2.5%/ps are tabulated in Table I. An abrupt increase of T_{BDT} can be seen with the increase in the strain rate $\dot{\varepsilon}$ indicating an exponential variation. The values of T_{BDT} obtained from this work are in the consistent range of values as predicted for bulk GaN.[37] T_{BDT} is observed to increase with increase in the strain rate, which indicates that, as the rate of applied tensile loading is increased, the brittle nature is maintained till the higher temperatures in order to keep the enthalpy constant. The corresponding logarithmic variation of $\ln\dot{\varepsilon}$ with inverse of T_{BDT} is shown in Fig. 4(c) which represents that the value of T_{BDT} shifts to the higher values with the increase in rate of applied tensile loading. The linear dependency is consistent with the prediction of Eq. (10). Further, the slope of this Arrhenius plot corresponds to the activation energy for the dislocation glide ΔH_d, as predicted first for silicon by John[38] by applying the theory of mobility of dislocations. The value of ΔH_d thus obtained is approximately 2.0 ± 0.05 eV for the present case, suggesting that the brittle to ductile transition is controlled by the dislocation mobility as in the case of other semiconductors like silicon and germanium.[39,40] The phenomenological quantity T_{BDT} depends on the initial test conditions, such as the geometry of the specimen, the method of applying the force, the strain rate, and also the environmental conditions. Below T_{BDT}, the material is brittle and above which plastic deformation takes place for a given strain rate.

Thermal conductivity as a function of temperature for both pristine GaN-ML and the (25,0) nanotube is shown in Fig. 5. The results indicate that the thermal conductivity decreases with the increase in temperature for both the structures. A rapid reduction can also be seen at the initial temperatures and then saturating at higher temperatures. Compared to the thermal conductivity of bulk GaN, the values are observed to be decreased for the (25,0) nanotubes. This observation is consistent with the results observed previously by Wang *et al.*[17] by using non-equilibrium molecular dynamics. The results are in close agreement with that of Wang *et al.* for the nanotube of thickness 0.37 nm at 600 K. Such a reduction of κ as compared to the bulk values has also been reported previously for GaN nanowires by means of experiments.[41] Moreover, a similar characteristic reduction of κ at the higher temperatures was observed experimentally for bulk GaN.[42] The values of κ are further reduced in the case of pristine GaN-ML, which could be understood due to the difference in surface-to-volume ratio. The reduction of κ as compared to the bulk GaN may be attributed to the fact that, due to the small size effects, increased phonon-phonon interactions result in the increased thermal resistance, thereby decreasing the conductivity.[43] The reduction in κ at

TABLE I. T_{BDT} (in K) at various strain rates (in%/ps).

$\dot{\varepsilon}$	0.10	0.40	0.89	1.6	2.5
T_{BDT}	833.33	1176.47	1250.00	1333.33	1666.67

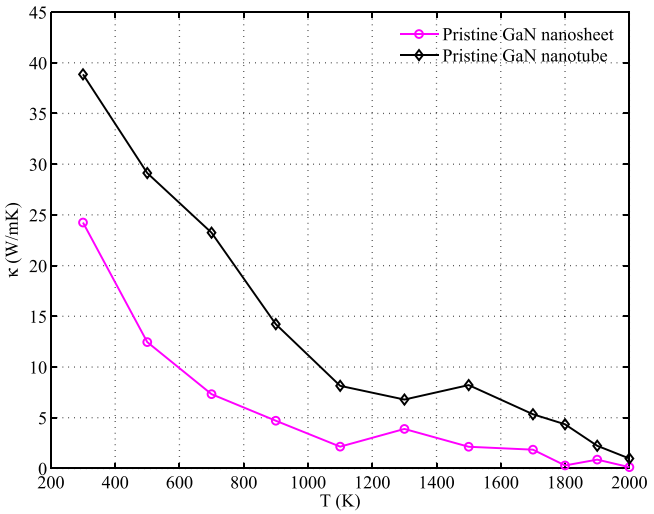

FIG. 5. The variation of thermal conductivity of GaN-ML in the temperature range of 300 to 2000 K. A rapid reduction in thermal conductivity that saturates at higher temperatures can be seen. At higher temperatures, the increased phonon-phonon interactions and the inelastic boundary scattering reduce the mean free paths. The results are compared with the (25,0) nanotube generated from the same GaN-ML.

higher temperatures could be the result of surface inelastic scattering and the reduced mean free path due to the dominant high frequency acoustic and optical phonon interactions. It was shown recently by theoretical investigation that, phonon confinement effect plays the major role in changing the phonon dispersion spectrum from that of bulk, resulting in much reduced phonon group velocity, leading to a significant reduction in thermal conductivity.[44] It was also shown there that, in the longitudinal acoustic phonon dispersion modes, the phonon confinement effect enhances the spacing between the adjacent branches, as the thickness of the nanotube is decreased. This accounts for the much more reduction in κ for monolayer.

IV. CONCLUSIONS

MD simulations on a system of GaN-ML are performed to study the mechanical behavior under tensile loading as a function of temperature. The fracture stress decreases with increasing temperature and finally a zig-zag type of variation in the behavior was observed at higher temperatures that indicate the onset of ductile failure. The temperatures at which brittle to ductile transition occur are obtained from the $\ln(\tau_y)$ versus $1/T$ plots for different strain rates and also compared for the GaN-ML in the presence of single and diatomic vacancies. The values of T_{BDT} thus obtained are used to plot $\ln \dot{\varepsilon}$ as a function of $1/T_{BDT}$ and the linear behavior observed from such an Arrhenius characteristic qualitatively agree well as predicted from the presented models. The value of activation energy of dislocation glide that is equivalent to the slope of such a plot is approximately 2.0 ± 0.05 eV for the present case, suggesting that the brittle to ductile transition is controlled by the dislocation mobility as in the case of other semiconductors like silicon and germanium. GK formulations have been employed to study the variation of thermal conductivity as a function of temperature. Thermal conductivity was observed to reduce rapidly at higher temperatures. High frequency phonon interaction spectrum and the surface inelastic scattering could be the cause of reduction in the thermal conductivity at high temperatures, whereas the small size effects may be attributed to be responsible for the reduction of κ as compared to that of bulk GaN case. Studies on thermomechanical behavior of a single layer semiconducting system would be of interest particularly while designing the nanoenergy conversion devices that benefit from the increased figure of merit.

ACKNOWLEDGMENTS

J.V.N. gratefully acknowledges the support from Dr. B. D. Pant, Dr. V. K. Khanna, and Dr. Chandra Shekhar (Director), of CSIR-CEERI, Pilani, India, by providing the study leave to carry out this work at IIT-R and thankful to the Institute Computer Center at IIT-R, for the computational facilities.

[1]C. Zhi, Y. Bando, C. Tang, H. Kuwahara, and D. Golberg, "Large-scale fabrication of boron nitride nanosheets and their utilization in polymeric composites with improved thermal and mechanical properties," Adv. Mater. **21**, 2889–2893 (2009).
[2]H. Zeng, C. Zhi, Z. Zhang, X. Wei, X. Wang, W. Guo, Y. Bando, and D. Golberg, "White graphenes':boron nitride nanoribbons via noron nitride nanotube unwrapping," Nano Lett. **10**, 5049–5055 (2010).
[3]D. Golberg, Y. Bando, Y. Huang, T. Terao, M. Mitome, C. Tang, and C. Zhi, "Boron nitride nanotubes and nanosheets," ACS Nano **4**, 2979–2993 (2010).
[4]C. Tusche, H. L. Meyerheim, and J. Kirschner, "Observation of depolarized ZnO(0001) monolayers: Formation of unreconstructed planar sheets," Phys. Rev. Lett. **99**, 026102 (2007).
[5]O. Altuntasoglu, Y. Matsuda, S. Ida, and Y. Matsumoto, "Syntheses of zinc oxide and zinc hydroxide single nanosheets," Chem. Mater. **22**, 3158–3164 (2010).
[6]M. Osada and T. Sasaki, "Exfoliated oxide nanosheets: new solution to nanoelectronics," J. Mater. Chem. **19**, 2503–2511 (2009).
[7]J. N. Coleman, M. Lotya, A. O'Neill, S. D. Bergin, P. J. King, U. Khan, K. Young, A. Gaucher, S. De, R. J. Smith, I. V. Shvets, S. K. Arora, G. Stanton, H. Y. Kim, K. Lee, G. T. Kim, G. S. Duesberg, T. Hallam, J. J. Boland, J. J. Wang, J. F. Donegan, J. C. Grunlan, G. Moriarty, A. Shmeliov, R. J. Nicholls, J. M. Perkins, E. M. Grieveson, K. Theuwissen, D. W. McComb, P. D. Nellist, and V. Nicolosi, "Two–dimensional nanosheets produced by liquid exfoliation of layered materials," Science **331**, 568–571 (2011).
[8]K. S. Novoselov, A. K. Geim, S. V. Morozov, D. Jiang, Y. Zhang, S. V. Dubonos, I. V. Grigorieva, and A. A. Firsov, "Electric field effect in atomically thin carbon films," Science **306**, 666–669 (2004).
[9]M. Osada and T. Sasaki, "Two-dimensional dielectric nanosheets: Novel nanoelectronics from nanocrystal building blocks," Adv. Mater. **24**, 210–228 (2012).
[10]Q. H. Wang, K. Kalantar-Zadeh, A. Kis, J. N. Coleman, and M. S. Strano, "Electronics and optoelectronics of two-dimensional transition metal dichalcogenides," Nat. Nanotechnol. **7**, 699–712 (2012).
[11]K. A. N. Duerloo, M. T. Ong, and E. J. Reed, "Intrinsic piezoelectricity in two-dimensional materials," J. Phys. Chem. Lett. **3**, 2871–2876 (2012).
[12]K. Ariga, Q. Ji, J. P. Hill, Y. Bando, and M. Aono, "Forming nanomaterials as layered functional structures toward materials nanoarchitectonics," NPG Asia Mater. **4**, e17 (2012).
[13]J. Goldberger, R. He, Y. Zhang, S. Lee, H. Yan, H.-J. Choi, and P. Yang, "Single-crystal gallium nitride nanotubes," Nature **422**, 599–602 (2003).
[14]T.-W. Yeh, Y.-T. Lin, B. Ahn, L. Stewart, P. Daniel Dapkus, and S. Nutt, "Vertical nonpolar growth templates for light emitting diodes formed with GaN nanosheets," Appl. Phys. Lett. **100**, 033119 (2012).
[15]L. D. Hicks and M. S. Dresselhaus, "Thermoelectric figure of merit of a one–dimensional conductor," Phys. Rev. B **47**, 16631–16634 (1993).

[16]Z. Wang, X. Zu, F. Gao, and W. J. Weber, "Atomistic simulation of brittle to ductile transition in GaN nanotubes," Appl. Phys. Lett. **89**, 243123 (2006).
[17]Z. Wang, F. Gao, J.-P. Crocombette, X. T. Zu, L. Yang, and W. J. Weber, "Thermal conductivity of GaN nanotubes simulated by nonequilibrium molecular dynamics," Phys. Rev. B **75**, 153303 (2007).
[18]E. Li, L. Hou, Z. Cui, D. Zhao, M. Liu, and X. Wang, "Electronic structures and transport properties of single crystalline gan nanotubes," Nano **07**, 1250014 (2012).
[19]Q. Chen, H. Hu, X. Chen, and J. Wang, "Tailoring band gap in GaN sheet by chemical modification and electric field: Ab initio calculations," Appl. Phys. Lett. **98**, 053102 (2011).
[20]L. Boldrin, F. Scarpa, R. Chowdhury, and S. Adhikari, "Effective mechanical properties of hexagonal boron nitride nanosheets," Nanotechnology **22**, 505702 (2011).
[21]J. V. N. Sarma, R. Chowdhury, and R. Jayaganthan, "Mechanical behavior of gallium nitride nanosheets using molecular dynamics," Comput. Mater. Sci. **75**, 29–34 (2013).
[22]X. W. Zhou, R. E. Jones, and S. Aubry, "Molecular dynamics prediction of thermal conductivity of GaN films and wires at realistic length scales," Phys. Rev. B **81**, 155321 (2010).
[23]S. Plimpton, "Fast parallel alogorithms for short-range molecular dynamics," J. Comput. Phys. **117**, 1–19 (1995).
[24]A. Bere and A. Serra, "On the atomic structures, mobility and interactions of extended defects in GaN: Dislocations, tilt and twin boundaries," Philos. Mag. **86**, 2159–2192 (2006).
[25]F. H. Stillinger and T. A. Weber, "Computer simulation of local order in condensed phases of silicon," Phys. Rev. B **31**, 5262–5271 (1985).
[26]W. G. Hoover, "Canonical dynamics: Equilibrium phase-space distributions," Phys. Rev. A **31**, 1695–1697 (1985).
[27]H. Zhao and N. R. Aluru, "Temperature and strain-rate dependent fracture strength of graphene," J. Appl. Phys. **108**, 064321 (2010).
[28]S. N. Zhurkov, "Kinetic concept of the strength of solids," Int. J. Fract. Mech. **1**, 311–322 (1965).
[29]A. I. Slutsker, V. I. Betekhti, J. C. Lee, D. Yusupov, A. G. Kadomtsev, and O. V. Amosova, "Temperature dependence of rupture strength of the amorphous alloy $Ni_{82.1}Cr_{7.8}Si_{4.6}Fe_{3.1}Mn_{0.3}Al_{0.1}Cu_{<0.1}B_2$," Acta Mater. **52**, 2733–2738 (2004).
[30]N. M. Pugno and R. S. Ruoff, "Quantized fracture mechanics," Philos. Mag. **84**, 2829–2845 (2004).
[31]T. L. Anderson, *Fracture Mechanics: Fundamentals and Applications*, 2nd ed. (CRC, Boca Raton, 1995).
[32]P. Pirouz, M. Zhang, J. L. Demenet, and H. M. Hobgood, "Yield and fracture properties of the wide band-gap semiconductor 4H-SiC," J. Appl. Phys. **93**, 3279–3290 (2003).
[33]Z. Ni, H. Bu, M. Zou, H. Yi, K. Bi, and Y. Chen, "Anisotropic mechanical properties of graphene sheets from molecular dynamics," Physica B **405**, 1301–1306 (2010).
[34]B. Mortazavi and Y. Rémond, "Investigation of tensile response and thermal conductivity of boron-nitride nanosheets using molecular dynamics simulations," Physica E (Amsterdam) **44**, 1846–1852 (2012).
[35]J. P. Hirth and J. Lothe, *Theory of Dislocations*, 2nd ed. (Wiley, New York, 1982), p. 531.
[36]P. Borvin, J. Rabier, and H. Garem, "Plastic deformation of GaAs single crystals as a function of electronic doping II: Low temperatures (20–300°C)," Philos. Mag. A **61**, 647–672 (1990).
[37]Y. Kamimura, H. Kirchner, and T. Suzuki, "Yield strength and brittle-to-ductile transition of boron-nitride and gallium-nitride," Scr. Mater. **41**, 583–587 (1999).
[38]C. S. John, "The brittle-to-ductile transition in pre-cleaved silicon single crystals," Philos. Mag. **32**, 1193–1212 (1975).
[39]B. J. Gally and A. Argon, "Brittle-to-ductile transitions in the fracture of silicon single crystals by dynamic crack arrest," Philos. Mag. A **81**, 699–740 (2001).
[40]F. C. Serbena and S. G. Roberts, "The brittle-to-ductile transition in Germanium," Acta metall. mater. **42**, 2505–2510 (1994).
[41]C. Guthy, C. Y. Nam, and J. E. Fischer, "Unusually low thermal conductivity of gallium nitride nanowires," J. Appl. Phys. **103**, 064319 (2008).
[42]H. Shibata, Y. Waseda, H. Ohta, K. Kazumasa, S. Kenji, K. Fujito, H. Nagaoka, Y. Kagamitani, R. Simura, and T. Fukuda, "High thermal conductivity of gallium nitride (GaN) crystals grown by HVPE process," Mater. Trans. **48**, 2782–2786 (2007).
[43]L. H. Liang and B. Li, "Size-dependent thermal conductivity of nanoscale semiconducting systems," Phys. Rev. B **73**, 153303 (2006).
[44]G. Zhou and L. Li, "Phonon thermal conductivity of GaN nanotubes," J. Appl. Phys. **112**, 014317 (2012).